ELSEVIER

Polymer 43 (2002) 2845–2859

polymer

www.elsevier.com/locate/polymer

Photopolymerization-induced phase separation in binary blends of photocurable/linear polymers

Kazutaka Murata[a], Jain Sachin[b,1], Hideki Etori[a], Takanori Anazawa[a,*]

[a]*Kawamura Institute of Chemical Research, 631 Sakado, Sakura, Chiba 285-0078, Japan*
[b]*Institute of Polymer Engineering, University of Akron, Akron, OH 44325, USA*

Received 31 August 2001; received in revised form 5 December 2001; accepted 19 December 2001

Abstract

Phase separation behavior and morphology of polymer blends induced by photopolymerization have been investigated in a binary blend of photocurable polymer (2,2-bis(4-(acryloxy diethoxy)phenyl)propane; BPE4) and linear polymer (polysulfone; PSU) using electron microscopy techniques. A ternary phase diagram of mono-BPE4/poly-BPE4/PSU exhibits a lower critical solution temperature (LCST) behavior. In situ polymerization of BPE4 over a wide range of PSU compositions (5–70 wt%) results in network-like bicontinuous phase separated structures at high temperatures, while semi-interpenetrating polymer network (IPN) structures are cured at low temperatures. Even at 10 wt% PSU, the PSU-rich phase is a continuous network-like phase. BPE4-rich domains in the network-like structures are controlled from the nanoscale (30 nm) to the microscale (1 μm) by varying the composition, curing temperature and irradiation intensity. By means of time-evolution study of the phase structure, it is found that BPE4-rich domains appeared in a PSU-rich matrix after the induction time. These domains quickly grow in size up to the sub-micron level, but further growth appears to be slow. The PSU-rich matrix develops into the network-like pattern by the increase in the number and growth of the BPE4-rich domains.

Keywords: Viscoelastic phase separation; Photochemical reaction; Photocurable polymer

1. Introduction

Phase separations associated with chemical reactions of reactive monomers have many and varied potential applications as systems because the initial homogeneous mixtures are easily provided compared with polymer/polymer systems. Numerous reports have been published on morphologies [1–6], phase separation behavior [1,2,5–10] and mechanical properties [1–3,11–14] in thermoset/thermoplastic polymers systems. Recently, it has been found that these phase separations with chemical reactions of reactive monomers also fall under the category of so-called viscoelastic phase separation [15]. Tanaka reported that in binary blend systems having very strong asymmetry in molecular dynamics such as polymer/solvent systems [16–19] and polymer/polymer systems having a very large difference in glass transition temperatures [20], the viscoelastic effect (polymer effect) plays a dominant role in phase separation behavior and unusual phase separation phenomena can be observed. Domains of a small molecule-rich phase appear in a polymer-rich matrix, and then network-like or sponge-like structures are formed by the domain growth. Finally, a continuous polymer-rich phase develops into a dispersed phase by shrinkage of the polymeric phase. In these systems, even a minor polymeric component provides network-like continuous phase separated patterns. Indeed, connected globule bicontinuous phase structures are given in the blend of thermoset/thermoplastic polymers with small amount of thermoplastic polymers, which brought about excellent mechanical properties [1–5]. Furthermore, unusual phase separation phenomena, in which droplet structures developed into bicontinuous structures, are also reported [21,22].

Recently photoirradiation curing systems have found various applications in coatings, inks and adhesion due to desirable features such as no-solvent, rapid cure and cold cure. Photochemical reaction systems have advantages over thermal reaction systems in controlling the phase structures, since the curing temperature and light intensity can be varied independently [23]. However, there has been little investigation of photopolymerization curing associated with polymer blends [23–25].

* Corresponding author. Tel.: +81-43-498-2135; fax: +81-43-498-2565.
E-mail address: takanori-anazawa@ma.dic.co.jp (T. Anazawa).
[1] Present address: Department of Polymer Technology, Eindhoven University of Technology, Den Dolech 2, STO 0.45, P.O. Box 513, Eindhoven, The Netherlands.

0032-3861/02/$ - see front matter
PII: S0032-3861(02)00056-3

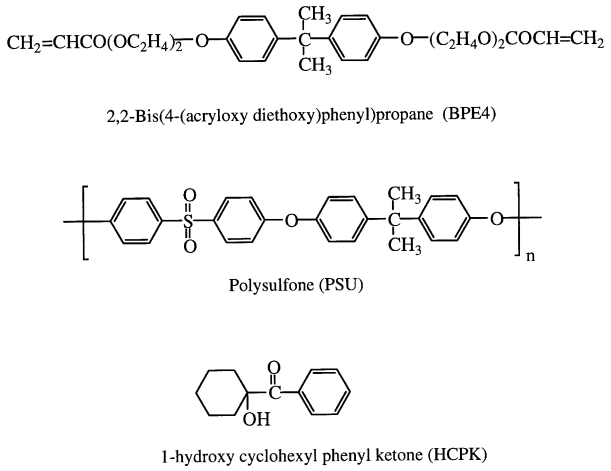

Fig. 1. Chemical structures of a photocurable monomer (BPE4), linear polymer (PSU) and photoinitiator (HCPK).

Here we report on phase structures controlled by photopolymerization curing in a binary blend of photocurable/linear polymers, and dependence of phase morphologies on blend compositions, polymerization temperatures and light intensities. Moreover, morphology development of the blend during photopolymerization was directly observed by electron microscopy.

2. Experimental

2.1. Materials

The sample of 2,2-bis(4-(acryloxy diethoxy)phenyl)propane (BPE4) supplied by Daiichi Seiyaku Kougyo Co., Japan, was used as the photocurable monomer. The linear polymer was polysulfone (PSU, Udel P-3703) obtained from Amoco Chemicals. Purified PSU was obtained by precipitating it from dichloromethane solution (ca. 2 wt% concentration) with an excess volume of methanol. The weight average molecular weight (M_w) of the purified PSU was 44,300, and the ratio between the weight average and number average molecular weights (M_w/M_n) was 1.90. The sample of 1-hydroxycyclohexylphenyl ketone (HCPK, Irgacure 184) obtained from Ciba Specialty Chemicals was used as the photoinitiator. To BPE4 was added 2 wt% (0.5 mol%) of HCPK (BPE4/HCPK) = (98/2 w/w). The chemical structures of BPE4, PSU and HCPK are shown in Fig. 1.

2.2. Photopolymerization-induced phase separation

A typical procedure for photoinduced phase separation is as follows. BPE4 (9 g), including 2 wt% HCPK (0.18 g), and PSU (1 g) were dissolved in methylene chloride (30 g) (for 10 wt% PSU composition). The samples were prepared by solvent casting on glass slides and were kept at room temperature (25 °C) overnight. Next, these solvent cast films were dried in a vacuum oven at 50 °C for 1 h. TGA measurement showed residual solvent in solvent cast films well below 0.1 wt% after drying. In this study, all coatings with 1–80 wt% PSU before the photopolymerization were transparent and homogeneous over a temperature range of 0–200 °C. The coating sandwiched between two glass slides containing spacers (PET films) with a thickness of 100 μm was heated at an appropriate temperature on a heat stage and then irradiated with ultraviolet (UV) light for 90–120 s using a high-pressure Hg-lamp (Spot Cure 250, Ushio Electric, Japan). UV intensity at the surface of the coating was ca. 10 mW cm^{-2} at 365 nm. The photopolymerization of BPE4 predominantly proceeds by the spectrum at 365 nm due to the use of HCPK as the photoinitiator. Phase separation takes place with the increase in the molecular weight of BPE4. Increase in molecular weight decreases the miscibility of one component in the other. Furthermore, vitrification and gelation due to the in situ cross-linking polymerization simultaneously suppresses the process of the phase decomposition. The coating was further cured by photoirradiation at 25 °C (room temperature) for 90 s under nitrogen atmosphere to ensure complete curing using a high-power UV light, a 3 kW metal–halide lamp (UE031, Eye Graphics, Japan); light intensity at 365 nm was ca. 75 mW cm^{-2}. Additional photoirradiation at room temperature virtually does not affect the earlier formed phase morphologies, since the post curing of the coatings, before additional irradiation, was done at temperatures well below the glass transition temperatures (T_g) of the coatings. In the case of 10 wt% PSU, T_gs before the post curing were above 50 °C.

2.3. Measurements

Phase separated morphology in the blend was observed using transmission electron microscopy (TEM) with a JEM-200CX (JEOL, Japan) and scanning electron microscopy (SEM) with a FE-SEM S-800 (Hitachi, Japan). For TEM observation, the cross-sections of the specimens (ca. 100 μm thickness) were microtomed into ultrathin sections of ca. 50 nm thickness and observed without staining. For SEM observation, the specimens (ca. 100 μm thickness) were fractured in liquid nitrogen and the PSU-rich phase was etched out with dichloromethane. The fractural surface was coated with platinum at a thickness of 5 nm. All micrographs of phase structures were taken from core regions in the coatings. We observed phase structures at different areas in the coatings by SEM and found that phase structures (morphology and size) did not vary much in the section except for the skin area at the surface.

The extent of curing of BPE4 in blends was estimated by Fourier-transform infrared spectroscopy (FT-IR) using a FT-IR-550 (JSCO, Japan). Conversions were calculated from the area [$(A_{805})_{t=0}$ and $(A_{805})_t$] of the absorption of the reactive acrylate functional groups at 805 cm^{-1} (CH_2=CH twisting) in the blends before and after photoirradiation

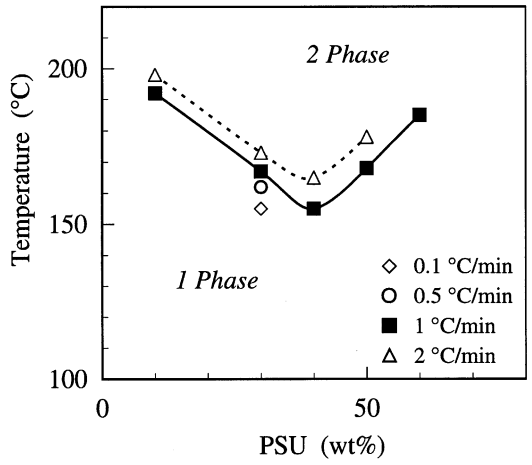

Fig. 2. Cloud-point curves for BPE4/PSU blends that were obtained from homogeneous mixtures of BPE4-monomer and PSU by heating at a ratio of (■) 1 °C min^{-1}, (△) 2 °C min^{-1}, (○) 0.5 °C min^{-1} and (◇) 0.1 °C min^{-1}.

[26]. The conversion (R_c (%)) of BPE4 is given by $[1-(A_{805}/A_{1732})_t/(A_{805}/A_{1732})_{t=0}]\times 100$, where $(A_{1732})_{t=0}$ and $(A_{1732})_t$ are the area of the absorption of the no reactive ester functional groups at 1732 cm^{-1} (C=O stretching) in the blends before and after photoirradiation, respectively. FT-IR spectra of the blends were measured by the KBr method.

Glass transition temperatures (T_g) of partially cured coatings and homogeneous mixtures of BPE4-monomer and PSU were obtained from a differential scanning calorimeter (DSC) measurement at a heat scan rate of 10 °C min^{-1} under nitrogen atmosphere using a DSC-7 (Perkin Elmer).

Dynamic mechanical measurements were carried out on a dynamic viscoelastometer using a Solids Analyzer RSA-II (Rheometric Scientific, Inc.) for cured coatings and a

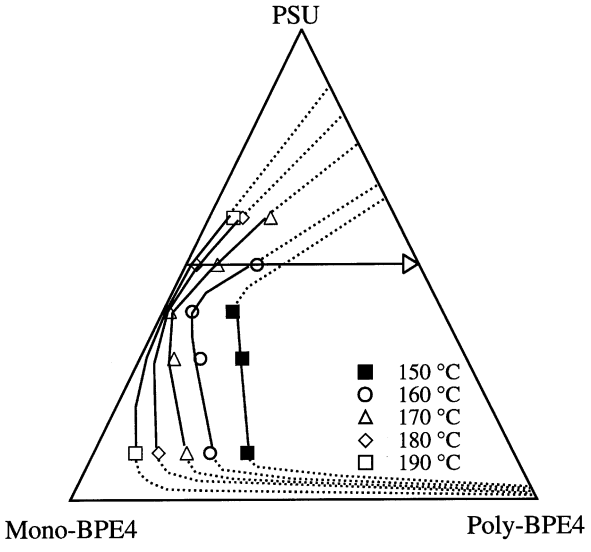

Fig. 3. Ternary phase diagram of the mono-BPE4/poly-BPE4/PSU system: coexistent lines at (■) 150 °C, (○) 160 °C, (△) 170 °C, (◇) 180 °C and (□) 190 °C. The arrow shows a reaction path at 50 wt% PSU.

Dynamic Analyzer RDS-II (Rheometric Scientific, Inc.) for viscoelastic fluids. Complex modulus E^* of coating films was measured at 1 Hz with a temperature sweep from 0 to 200 °C at a heating rate of 2 °C min^{-1}. T_g values of cured coatings refer to the maximum in the tan δ ($=E''/E'$) peak, where E' is the storage modulus and E'' is the loss modulus. For viscoelastic fluids, which are BPE4-monomer/PSU homogeneous mixtures before photoirradiation, complex shear modulus $G^*(i\omega)$ was measured on frequency sweeps from 100 to 0.1 rad s^{-1} with 10–50% strain at temperatures of 40–130 °C in a nitrogen atmosphere. Parallel plates (50 mm$^{\phi}$) with a gap of 1–2 mm were used.

We observed the transparency of coatings with a thickness of ca. 100 μm on a haze meter using an NDH-300A (Nippon Denshoku, Japan).

3. Results and discussion

3.1. Phase behavior in a ternary blend of mono-BPE4/poly-BPE4/PSU

All compositions of BPE4-monomer/PSU with 1–80 wt% PSU before photopolymerization were transparent and homogeneous over a temperature range of 0–200 °C. Phase separation in mixtures is induced by in situ polymerization of BPE4-monomer. We also observed that above 150 °C, BPE4 slowly polymerized due to thermal reaction. According to the data obtained from DSC measurement at a heating rate of 1 °C min^{-1}, the thermal reaction of BPE4 was initiated at around 154 °C. When the homogeneous and transparent coating of BPE4-monomer/PSU (7/3 w/w) was heated from 120 °C at the rate of 1 °C min^{-1}, the transparent blend coating became translucent at around 167 °C. We found that if it was quickly cooled, the translucent coating became transparent again. Fig. 2 shows cloud-point curves for BPE4/PSU blends, which were obtained from homogeneous mixtures of BPE4-monomer/PSU by uniform heating at a rate of 0.1–2 °C min^{-1}. The cloud-point curves exhibit a lower critical solution temperature (LCST) behavior. The lowest phase transition temperature is found at around 40 wt% PSU. In the case of 30 wt% PSU, the conversions of BPE4 at the cloud-points of 155 °C (heating ratio = 0.1 °C min^{-1}), 162 °C (0.5 °C min^{-1}), 167 °C (1 °C min^{-1}) and 173 °C (2 °C min^{-1}) were 35, 28, 16 and 5%, respectively. The cloud-point curve shifts to the low temperature region as the conversion of BPE4 increases. Two phases region broadens to the low-temperature region with polymerization. Fig. 3 shows the ternary phase diagram of the mono-BPE4/poly-BPE4/PSU system, where the molecular weight distributions were neglected. The arrow in Fig. 3 shows a reaction path of the blend at 50 wt% PSU. Phase separation should have been initiated at a lower polymerization degree as the curing temperature increased.

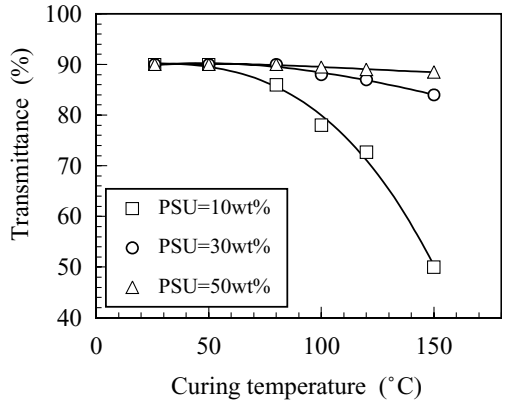

Fig. 4. Transmittance of coatings prepared by photopolymerization for BPE4/PSU systems as a function of cure temperature: (□) PSU = 10 wt%, (○) PSU = 30 wt% and (△) PSU = 50 wt%.

3.2. Morphology

BPE4/PSU blend coatings with different compositions were prepared by photopolymerization at 25–180 °C. Fig. 4 shows transmittance of the coatings as a function of curing temperature. In the case of the blends with 10% by weight of PSU, photopolymerization above 80 °C drastically decreased the transparency of the coatings from 90 to 50–80%, while in the blends with 30 wt% PSU, the transparency of the coatings decreased slightly from 90 to 85% when cured above 100 °C. In contrast, cured coatings with 50 wt% PSU were transparent over a wide range of curing temperatures of 25–180 °C. First, we investigated phase structures of the blends with a composition of 10% by weight of PSU, which became turbid due to curing at a high temperature.

3.2.1. Curing temperature dependence

Phase structures in the blends with 10 wt% PSU cured at 25–200 °C were observed by TEM. In all cases, the photopolymerizations were done at a temperature higher than T_g (−25 °C) of BPE4-monomer/PSU (9/1 w/w). Network-like phase separated patterns were observed by TEM for the blends cured above 50 °C, while phase structures were vague in the blends cured below 40 °C. The resultants are shown in Fig. 5. The dark part is the PSU-rich phase, and the bright part is the BPE4-rich phase. Interestingly, a minor component (PSU-rich phase) appeared as a network-like continuous interconnected structure. In TEM images (i.e. patterns in cross-section) microcells of the BPE4-rich part were wrapped continuously in all of the three dimensions, mostly with the PSU-rich phase, since the same network-like patterns in the TEM images were observed irrespective of the cutting direction of the coatings. Fig. 6 shows a SEM image of BPE4/PSU (9/1 w/w) blend cured at 120 °C. The PSU-rich phase was dissolved and etched out with dichloromethane, so the remaining phase should be a cross-linked BPE4-rich phase. Small spherical BPE4-rich particles were connected to one another, forming a three-dimensional network as observed from the SEM image. Consequently, a bicontinuous phase structure, i.e. both of the PSU-rich and BPE4-rich phases are continuous, has been formed. That it is a bicontinuous structure is supported by the fact that partially broken network-like patterns are found in TEM micrographs and also no powder was obtained after etching the coatings in dichloromethane. The small globule particles in the SEM image were uniform at a size of 0.4 μm, which corresponds to the BPE4-rich round domains in the TEM image (see Fig. 5(b)). Similar connected-globule structures were also observed in thermoset/thermoplastic polymer systems induced by thermal reaction [1–10].

Fig. 7 shows distribution curves of spherical BPE4-rich domain sizes in the blends with 10 wt% PSU. The BPE4-rich domain in the TEM image was referred to as either round or oval shapes. The BPE4-rich domain size was determined by taking a diameter for circles or by determining the mean value of the minor and major axis for ellipses. The distribution curve was given by normalized domain numbers (N_i/N_0) in increments of 0.05 μm, where N_0 is the total domain number in the TEM micrograph and N_i is the domain number in a range of i to $i + 0.05$ μm. In the blends cured above 150 °C, the distribution curves were divided into two curves below and above ca. 0.5 μm. Large domains above 0.5 μm occupy a major area in the blend. The peaks of the distribution curves above 0.5 μm shifted to a large domain region with the curing temperature. The peaks also lowered and broadened with the cure temperature. The curves below 0.5 μm give a maximum at 0.2 μm. Small domains are found in the remaining area of large domains, and they ought to be generated after the growth of the large domains. Disorder of the domain in the blends cured above 150 °C are probably caused by the time lag in generating a BPE4-rich domain, since phase separation and decreasing in miscibility proceed simultaneously. In the blends cured below 120 °C, the distribution curves gave a sharp shape with a small shoulder peak at around 0.2 μm. The distribution curves also shifted to a large domain region with the curing temperature.

Fig. 8 shows the relationships between the curing temperature and BPE4-rich domain size R_m. The domain sizes R_m in the network-like structures were given by the domain sizes at the peaks of the distribution curves. When two peaks appeared in the curve, the large one was used. The domain size R_m shows strong dependence on curing temperature. The BPE4-rich domain sizes in the network-like structures increased and also became disordered with curing temperature. The blend coating cured at 50 °C with phase structure below 0.2 μm was transparent. Temperature dependence of the domain sizes will be discussed later.

3.2.2. Composition dependence

Phase structures of BPE4/PSU blends with 1–70% by weight of PSU were investigated. Phase separated structures with sharp and clear boundaries were also observed in the blends cured in a high-temperature regime, whereas phase

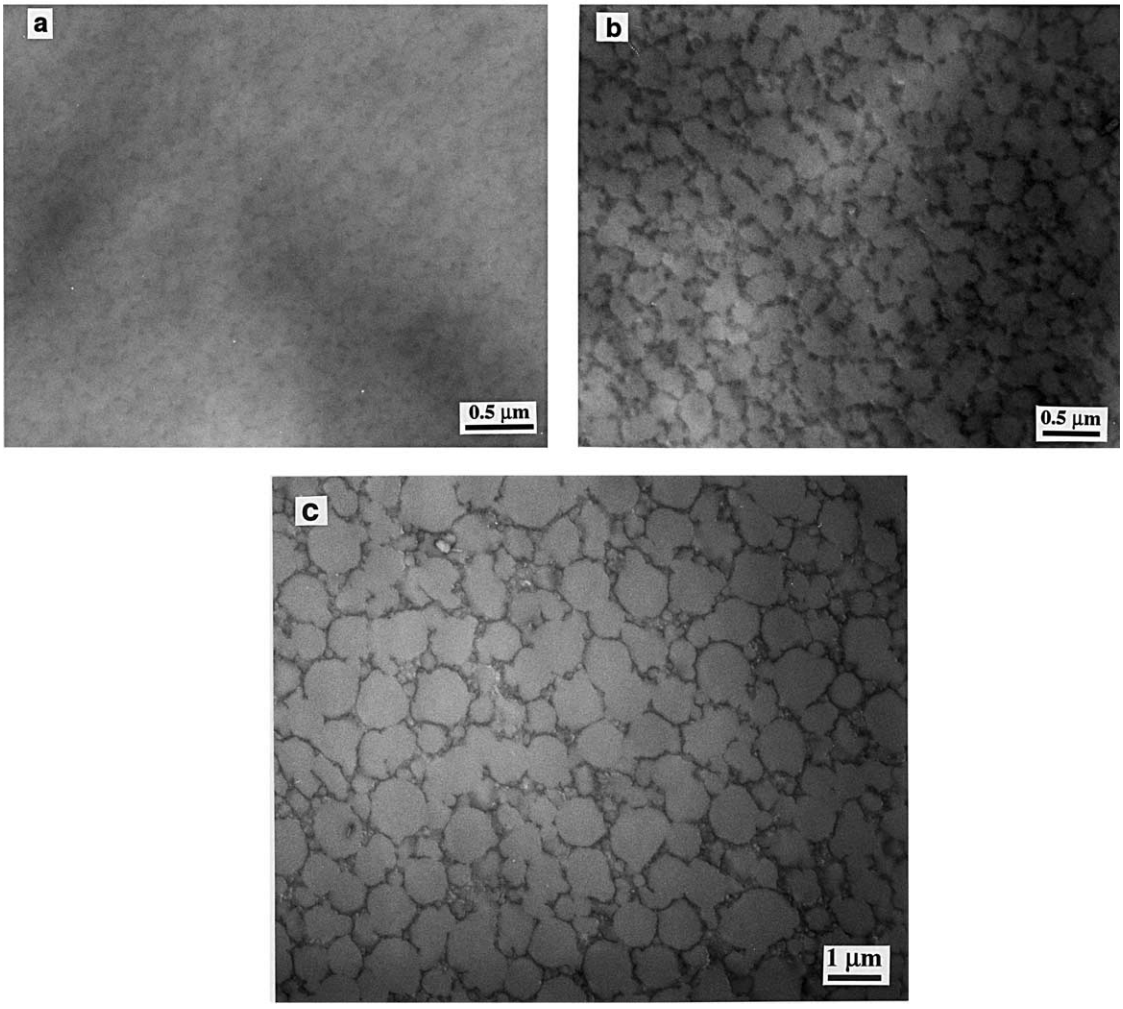

Fig. 5. TEM micrographs of phase structures for BPE4/PSU (9/1 w/w) prepared by photopolymerization at (a) 50 °C, (b) 120 °C and (c) 180 °C. The dark part of the figure is the PSU-rich phase, and the bright part is the BPE4-rich phase.

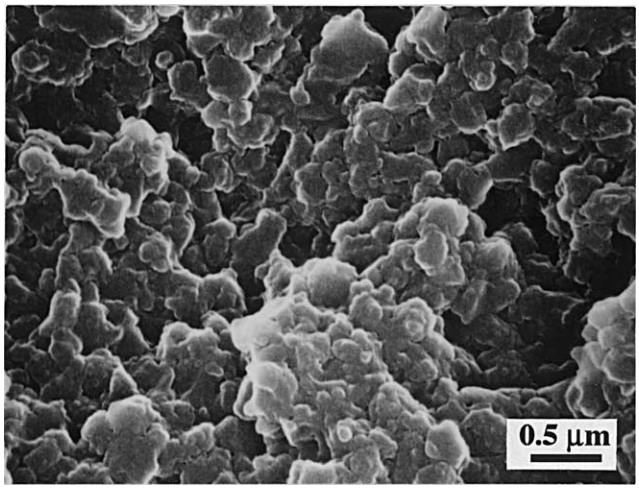

Fig. 6. SEM micrograph of the phase structure for BPE4/PSU (9/1 w/w) cured at 120 °C. PSU is washed out by etching with dichloromethane.

structures became vague with a diffused boundary when cured at a lower temperature. The boundary of curing temperature at which a phase separated structure appeared increased with PSU composition viz. 1–5 wt% (below 25 °C), 10 wt% (50 °C), 20 wt% (80 °C), 30 wt% (100 °C), 50 wt% (130 °C) and 70 wt% (180 °C) (see Fig. 14). The dependence of curing temperature on PSU composition can be attributed to low molecular mobility (high viscosity) at high PSU compositions. Zero shear viscosities of the homogenous mixtures before photoirradiation were 15 Pa s at 10 wt% PSU, 30 Pa s at 20 wt% and 120 Pa s at 30 wt% PSU at the boundary cure temperatures for the formation of the phase structure, which increased with PSU content. It may be that the diffusion length to form the phase structures decreased with PSU content.

Resulting morphologies are shown in Fig. 9. The network-like phase separated patterns appeared from the coating with 10–50 wt% PSU, while the PSU-rich phase formed a shred of network-like bicontinuous pattern at

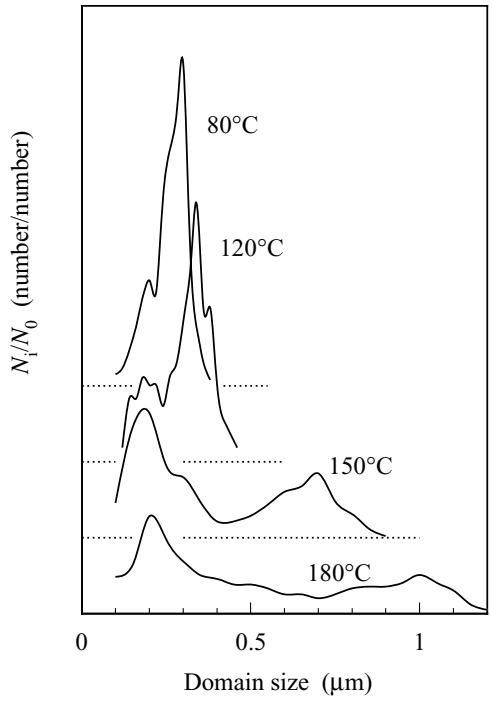

Fig. 7. Distribution curves of BPE4-rich domain sizes for BPE4/PSU (9/1 w/w) cured at 80, 120, 150 and 180 °C: N_0 is the total domain number in TEM image, and N_i is the domain number with sizes of $i \sim i + 0.05$ μm.

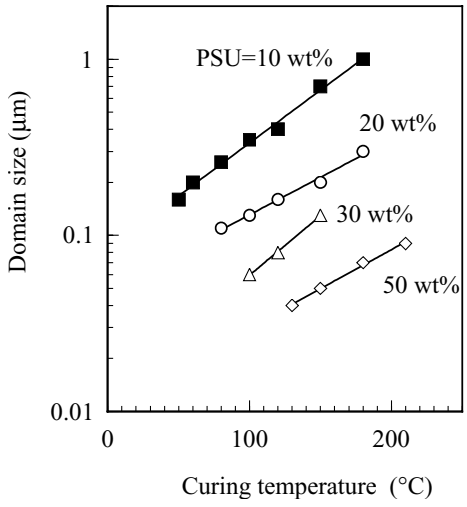

Fig. 8. Relationship between BPE4-rich domain size (R_m) and photocuring temperature for BPE4/PSU blends. R_m is given by the domain size at the peak of the distribution curve: (■) PSU = 10 wt%, (○) PSU = 20 wt%, (△) PSU = 30 wt% and (◇) PSU = 50 wt%.

5 wt% PSU. In the case of 1 and 70 wt% of PSU, droplet structures appeared. At 1 wt% PSU, the PSU-rich phase became islands dispersed in the BPE4 matrix. The domains were fairly uniform, with a size of 40–50 nm. This domain structure might be related to the moving droplet phase observed in polymer solution systems [15,16]. It is note worthy that phase inversion took place at an extremely symmetric composition of 2–5 wt% PSU, since a similar droplet structure was observed in the blend with 2 wt% PSU content. On the contrary, at 70 wt% PSU, the BPE4-rich phase was distributed as islands in the PSU-rich phase matrix. The domains were dispersed in sizes from 20 to 60 nm. Coatings with 70 wt% PSU were easily dissolved in dichloromethane due to the isolation of the BPE4-rich phase. Fig. 10 shows a SEM image of the fractured surfaces of the blend with 50 wt% PSU. Fine globule particles of the BPE4-rich phase were connected to one another at a uniform size of 60 nm, which corresponds to the domain sizes in the TEM image (see Fig. 9(c)). The BPE4-rich phase is also the same continuous phase as the PSU-rich phase. No globule particles were observed in the blend of 5 wt% PSU in the SEM observation.

The relationships of the spherical BPE4-rich domain sizes R_m at various compositions with curing temperatures can be established from Fig. 8. The domains significantly decreased with increasing PSU content. In the blends cured at 150 °C, the domain sizes R_m of the BPE4-rich phase were found to reduce from 0.7 to 0.2, 0.13 and 0.06 μm as the PSU composition increased from 10 to 20, 30 and 50 wt%, respectively. Notably, at 50 wt% PSU, the spherical domains were smaller than 100 nm, which was due to the fact that coatings at 50 wt% PSU remain transparent in spite of the formation of phase structures. It has also been reported that spherical domains decrease with the increase of a composition of polymeric component and with a decreasing cure temperature in thermal polymerization systems [3,4].

3.2.3. Dependence on light intensity

We investigated the effects of UV intensity on the phase structure using a high-power UV lamp (75 mW cm^{-2}), which is 7.5 times stronger than a Spot Cure UV lamp (10 mW cm^{-2}). Even with high-UV intensity, a network-like phase separated pattern appeared at high-temperature curing. At 10 wt% PSU, the spherical domain sizes R_m at 60, 80, 100, 120, 150 and 180 °C were ca. 0.1, 0.15, 0.25, 0.3 and 0.35 μm, respectively. Furthermore, at the curing temperature of 150 °C, the domain sizes R_m in the blends with 10, 20, 30 and 50 wt% PSU were ca. 0.3, 0.12 μm, ca. 80 and 30 nm, respectively. These values are 50 ± 10% of those with standard UV intensity (10 mW cm^{-2}).

Fig. 11 shows the relationships between the domain size R_m and UV intensity for 10 wt% PSU blends cured at 120 and 150 °C. UV intensity at the surface of the coating was controlled by band pass filters (Toshiba UV-D36B, $340 < \lambda < 370$ nm, transmittance at 365 nm = 50%). A plot of domain sizes R_m against UV intensity I on a log–log scale gives a straight line, as in Fig. 11. The relation was obtained as $R_m \sim R_0 I^{-a}$, and the exponent factors were 0.34 and 0.42 for the lines cured at 120 and 150 °C, respectively. The BPE4-rich domains R_m became smaller with light intensity. Furthermore, domains became fairly uniform at high-intensity curing. The relationship between domain sizes R_m and light intensity I is also discussed in a later section.

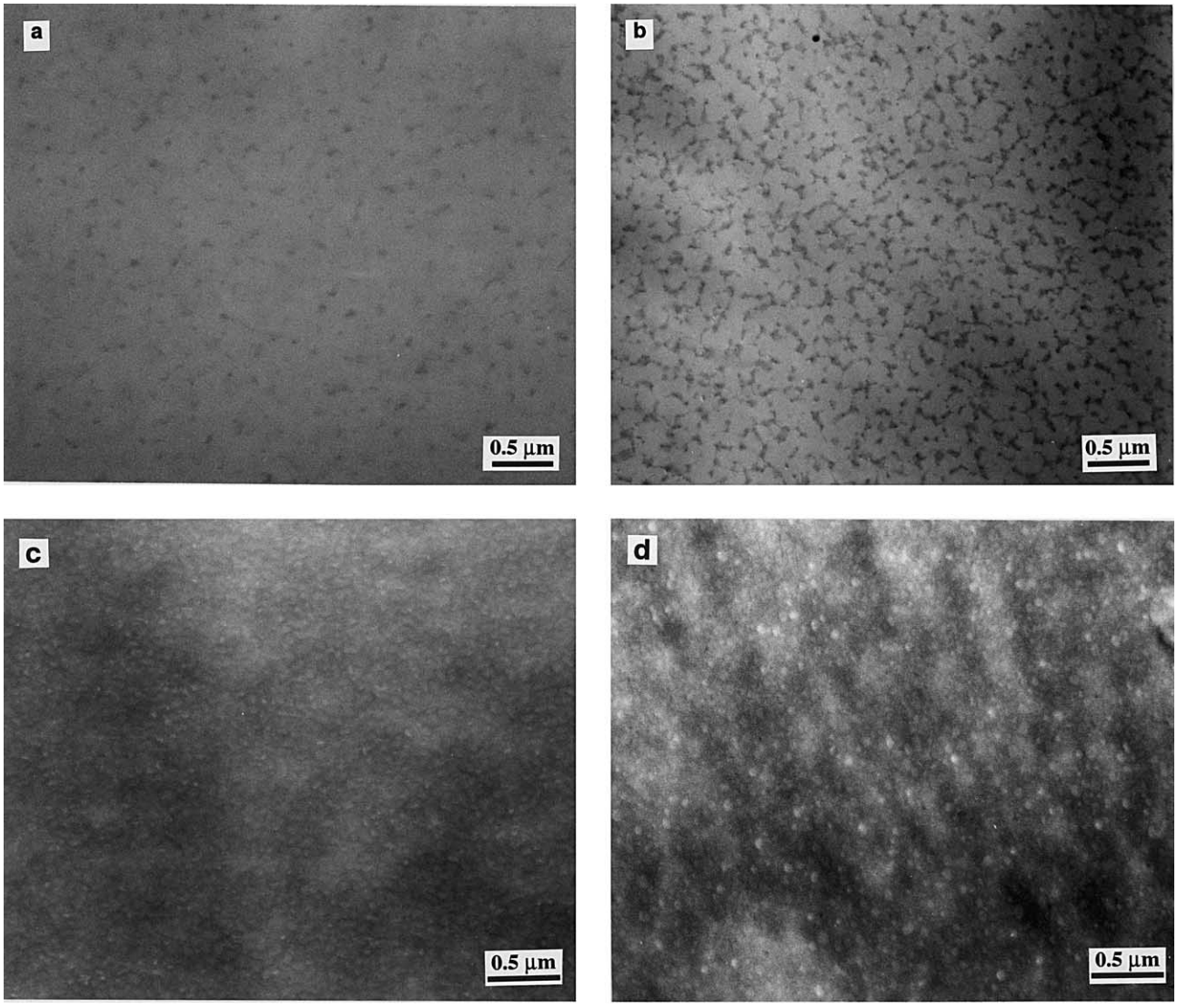

Fig. 9. TEM micrographs of phase structures for BPE4/PSU prepared by photopolymerization: (a) PSU = 1 wt% cured at 80 °C, (b) PSU = 5 wt% cured at 100 °C, (c) PSU = 50 wt% cured at 180 °C and (d) PSU = 70 wt% cured at 190 °C.

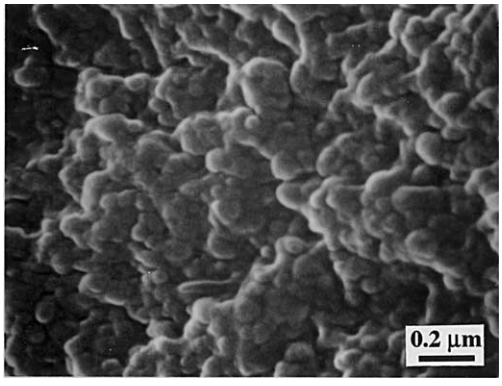

Fig. 10. SEM micrograph of phase structure for BPE4/PSU (5/5 w/w) cured at 180 °C. PSU is washed out by etching with dichloromethane.

It is very interesting to note that with 70 wt% PSU, a network-like phase separated pattern was obtained at high-UV intensity, while at lower intensity an island–sea structure appeared. The structure is shown in Fig. 12. The spherical domains in Fig. 12 were fairly uniform, with a size of 65 nm. When this coating cured at high irradiation intensity was dipped in dichloromethane, insoluble components remained. At 70 wt% PSU, the phase separation should proceed in the unstable region (spinodal region) by photopolymerization at 180 °C with an intensity of 75 mW cm^{-2}, which corresponds to the deep quench condition, while at 180 °C with an intensity of 10 mW cm^{-2} the decomposition process should be initiated in the metastable region (binodal region) by photopolymerization that corresponds to the shallow quench condition. It has been reported that the phase decompositions with slow chemical reactions are initiated in a metastable region and then enter an

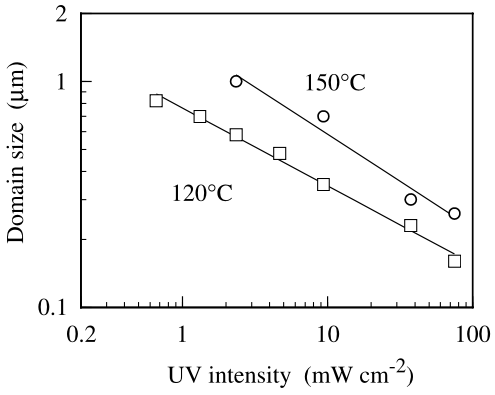

Fig. 11. Relationship between BPE4-rich domain sizes (R_m) and UV intensity (I) for BPE4/PSU (9/1 w/w) cured at (□) 120 °C and (○) 150 °C.

unstable region as the reaction proceeds, which is schematically shown in Fig. 13 [23,25]. However, in the blend with higher PSU content, it is possible that the resulting structure would have provided the premature phase separated morphology, since the phase decomposition is easy to freeze in the early stage due to the higher viscosity of the mixtures and the distant composition from the critical composition, at which the metastable region broadened and the polymerization degree induced decomposition becomes higher, as shown in Fig. 13. On the other hand, at low PSU composition, when chemical reaction becomes slow, the phase point tends to approach the coexisting line by phase decomposition due to low viscosity. In the case of the blend with 10 wt% PSU cured at 150 °C, sea–island phase separated structures with disordered large BPE4-rich droplets (>1 μm) appeared by photopolymerization with light intensities below 0.3 mW cm^{-2}.

Eventually, bicontinuous phase separated structures have been obtained by photopolymerization over a wide range of

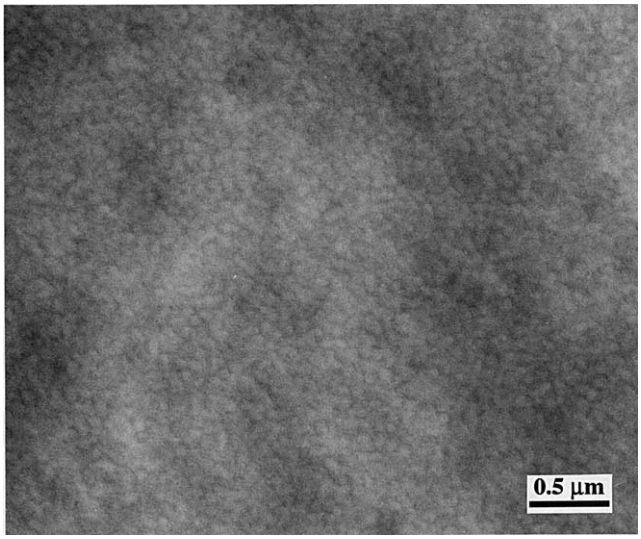

Fig. 12. TEM micrograph of phase structure for BPE4/PSU (3/7 w/w) cured at 190 °C with a light intensity of 75 mW cm^{-2}.

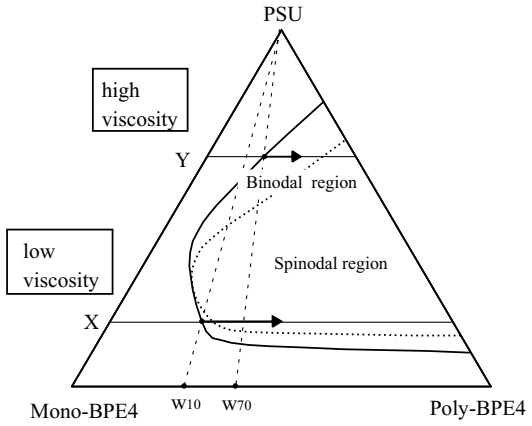

Fig. 13. Schematic ternary phase diagram for mono-BPE4/poly-BPE4/PSU. When phase separation is initiated in a metastable region (binodal region) under a shallow quench condition, phase decomposition is apt to enter an unstable region (spinodal region) with the polymerization at low PSU composition of X due to low viscosity and small w10, while suppressing the metastable region at high PSU composition of Y (Y > X) due to high viscosity and high w70; where w10 and w70 are initial molecular weight induced phase decomposition at PSU compositions of X and Y, respectively.

compositions of 5–70% by weight of PSU. In the case of high-UV intensity curing, the phase structures below 0.1 μm were provided in the blend in compositions of 30–70 wt% PSU.

3.2.4. Glass transition behavior in resulting structures

The effect of glass transition temperatures on the resulting blend coatings were investigated. Fig. 14 shows the temperature dependence of the storage modulus (E') and

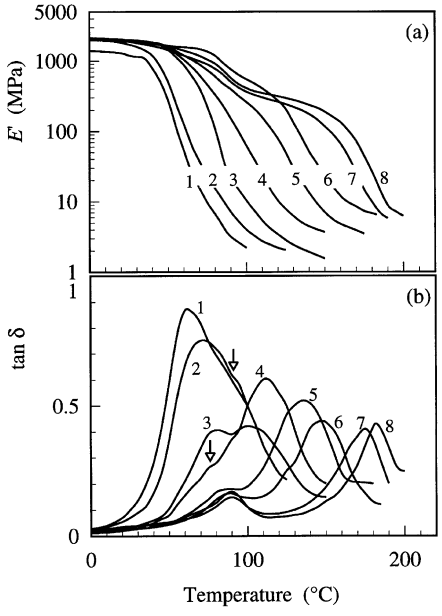

Fig. 14. Temperature dependence of (a) storage modulus (E') and (b) tan δ for BPE4/PSU (5/5 w/w) cured at (1) 25 °C, (2) 50 °C, (3) 80 °C, (4) 100 °C, (5) 120 °C, (6) 150 °C, (7) 180 °C and (8) 210 °C. Frequency = 1 Hz.

Table 1
Tan δ peak temperatures (T_g), conversion of BPE4 and calculated compositions of BPE4-rich and PSU-rich phases for BPE4/PSU (5/5 w/w) cured at 25–210 °C (T_g of neat PSU is 198 °C)

Curing temperature (°C)	T_g of cured BPE4 (°C)	Conversion (%)	T_g of BPE4/PSU (5/5 w/w)		Conversion (%)	Calculated compositions from the Fox relationship			
			BPE4-rich phase (°C)	PSU-rich phase (°C)		BPE4-rich phase		PSU-rich phase	
						BPE4 (%)	PSU (%)	BPE4 (%)	PSU (%)
25	62	85	61		65	–	–	–	–
50	67	88	71	85	70	96	4	83	17
80	80	92	81	99	78	97	3	80	20
100	82	93	84	109	82	98	2	71	29
120	86	94	86	136	85	98	2	52	48
150	86	94	89	148	87	97	3	38	62
180	86	95	89	174	88	97	3	16	84
210	87	95	89	182	89	98	2	11	89

tan δ for the blend coatings of BPE4/PSU (5/5 w/w) cured at temperatures of 25–210 °C with a light intensity of 10 mW cm^{-2}. Only one glass transition appeared as tan δ peak at around 61 °C by the photopolymerization at 25 °C, which is below T_g (45 °C) of the homogeneous mixture of BPE4-monomer/PSU (5/5 w/w). It is possible that a semi-interpenetrating polymer network (semi-IPN) structure would be given by the photopolymerization at 25 °C. Tan δ peak at 63 °C is considerably lower than the predicted glass transition temperature (ca. 120 °C) determined in the Fox relationship [27]. It should be ascribed to lower conversion of BPE4 (ca. 65%) in the blend cured at 25 °C. The conversion should be inevitably restricted by the formation of the semi-IPN structure, at which PSU molecules interpenetrate into a BPE4 cross-linked network.

In the tan δ curve of the blend cured at 50 °C, a main peak appeared at 71 °C and a shoulder peak was slightly observed at around 84 °C. There was no structure observed in this blend by TEM. Double peaks appeared on the tan δ curve in the blend cured at 80 °C, and a main tan δ peak in high-temperature region and shoulder in low-temperature region were observed in the blends cured at 100 and 120 °C. In the blends cured in a temperature range of 80–120 °C, the vague structures were observed. These vague phase structures should be fixed on a phase structure at a very early stage of the phase decomposition. The vitrification should be attributed to the quickly slowing phase separation rate as the system becomes viscous due to the low temperature region.

On the other hand, we observed two distinct glass transitions on the tan δ in the blends cured above 150 °C, corresponding to the clearly formed network-like structure. The T_gs in the low-temperature region appeared at around 89 °C in spite of the cure temperatures, which corresponds to T_g of the BPE4-rich phase. The composition of the BPE4-rich phase is found to be (BPE4/PSU) = (97/3 w/w) calculated from the Fox relationship, where the T_gs of cured BPE4 and PSU were 86 and 198 °C, respectively. T_gs of the PSU-rich phase in the high-temperature region increased with the curing temperature. The T_gs and calculated compositions are given in Table 1. The conversions of BPE4 in the blends with 50 wt% PSU cured above 150 °C were saturated at around 88%, and they are also shown in Table 1. The PSU composition in the PSU-rich phase increased with the curing temperature. The phase decomposition in the PSU-rich matrix phase further progresses with increase of the curing temperature, while the BPE4-rich domain can be estimated as a pure BPE4 phase independent of the curing temperature. In the blends cured above 150 °C, it is possible that the phase structure might be vitrified at the coexistent composition, since T_g of the PSU-rich phase in the blend cured at 150 °C were ca. 150 °C independent of light intensities of 5–75 mW cm^{-2}. In the blends cured below 120 °C, the BPE4 compositions in the PSU-rich phase were above 50 wt% by the calculation from the Fox relationship. It should also be attributed to the effect of the lower conversion of BPE4.

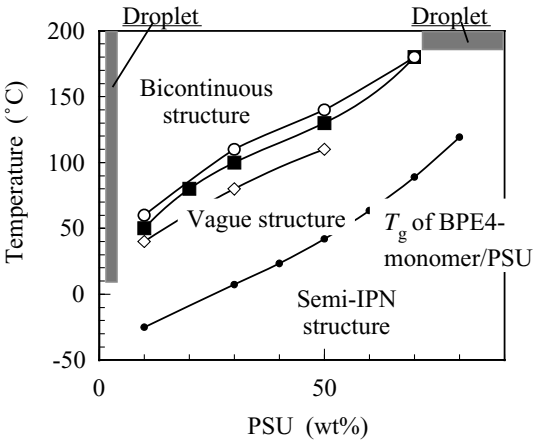

Fig. 15. Relationships between PSU content and T_{bi} for the BPE4/PSU system prepared by photopolymerization with light intensities of (◇) 1 mW cm^{-2}, (■) 10 mW cm^{-2} and (○) 75 mW cm^{-2}; T_{bi} is the curing temperature at which the network-like bicontinuous phase separated structure appeared. (·) T_g of BPE4-monomer and PSU homogeneous mixtures (T_{g0}).

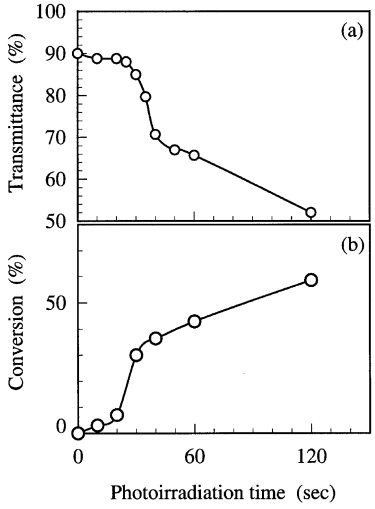

Fig. 16. Temporal changes of (a) transmittance and (b) conversion of BPE4 in the blend of BPE4/PSU (9/1 w/w) during photopolymerization at 150 °C with a light intensity of 1 mW cm^{-2}.

3.2.5. Summary of morphology control

The boundary cure temperatures (T_{bi}) at which the phase structures appeared are shown in Fig. 15. The glass transition temperature of the homogeneous mixture of BPE4-monomer/PSU (T_{g0}), before photoirradiation, is also shown in Fig. 15 as a function of PSU content. T_{bi} increased with the irradiation intensities, which were T_{g0} + 80 °C, T_{g0} + 90 °C and T_{g0} + 100 °C with light intensities of 1, 10 and 75 mW cm^{-2}, respectively.

Semi-IPN structures should be formed by photopolymerization at temperatures below the T_{g0}s. On the other hand, photoreaction at the intermediate temperature range of T_{g0} − T_{g0} + 80 °C results in vague, unclear structures. Droplet structures were given in extremely asymmetric blend compositions, which were below 2 wt% PSU and above 70 wt% PSU. PSU-rich domains were dispersed in a BPE4-rich matrix in the blends below 2 wt% PSU, while a BPE4-rich phase became islands in the PSU-rich matrix in the blends above 70 wt% PSU.

In photocurable/linear polymer systems, network-like bicontinuous structures can evolve as a result of a large variety of combinations as compared with polymer/polymer systems, since homogeneous mixtures are easily obtained due to the use of reactive monomers or oligomers. It has been confirmed that the network-like phase structures are also obtained in BPE4/polyarylate, BPE4/poly(methyl metacrylate), dimethyl tricyclodecane diacrylate/polycarbonate, 1.6-hexanediol diacrylate/polystyrene, trimethylol propane triacrylate/poly(vinyl chloride).

3.3. Evolution of phase structure with time during photopolymerization

Phase structures were concurrently quenched at different stages during the photopolymerization and observed by TEM to get direct representation. The cured blends with different photoirradiation time were obtained as follows. The homogenous coating of BPE4/PSU (9/1 w/w) sandwiched between two glass slides was heated on a heat stage at 150 °C. The coating was irradiated with low-power UV light (Spot Cue 250) for various time spans (t_{ir}). UV intensity at 365 nm was set at 1 mW cm^{-2} by controlling the distance between the UV lamp and the sample surface. The partially cured coating after the photoirradiation was quickly quenched in ice-water at 2 °C and then further cured in ice-water with the high-power UV light (UE031) at an intensity of 75 mW cm^{-2} at 365 nm for TEM observation.

Fig. 16 shows temporal changes of (a) transmittance and (b) conversion of BPE4 in the partially cured coatings during photopolymerization. T_g of the partially cured coatings could not be clearly observed at the early stage of the phase decomposition (t_{ir} < 37 s); however, the T_gs were above 40 °C for long periods of irradiation time, viz. longer than 40 s.

Time-resolved observation of phase structures during photopolymerization is shown in Fig. 17. There were no structures observed at the beginning of the reaction (t_{ir} < 30 s). BPE4-rich domains appeared in the PSU-rich matrix after the induction time; the induction time (30–32 s) corresponds to the time at which transparent coatings turn into turbid ones due to partial curing. The domains quickly nucleated up to ca. 0.5 μm, and then the development of the domain size became slow, appearing to reach saturation at around 0.5–0.6 μm (see Fig. 17(a)). This decrease in the domain growth rate should be attributed to viscoelastic effects in the polymeric phase [15–18]. The PSU-rich matrix phase developed into the network-like pattern with increasing number and growth of BPE4-rich domains with photoirradiation time. The matrix phase occupied a large

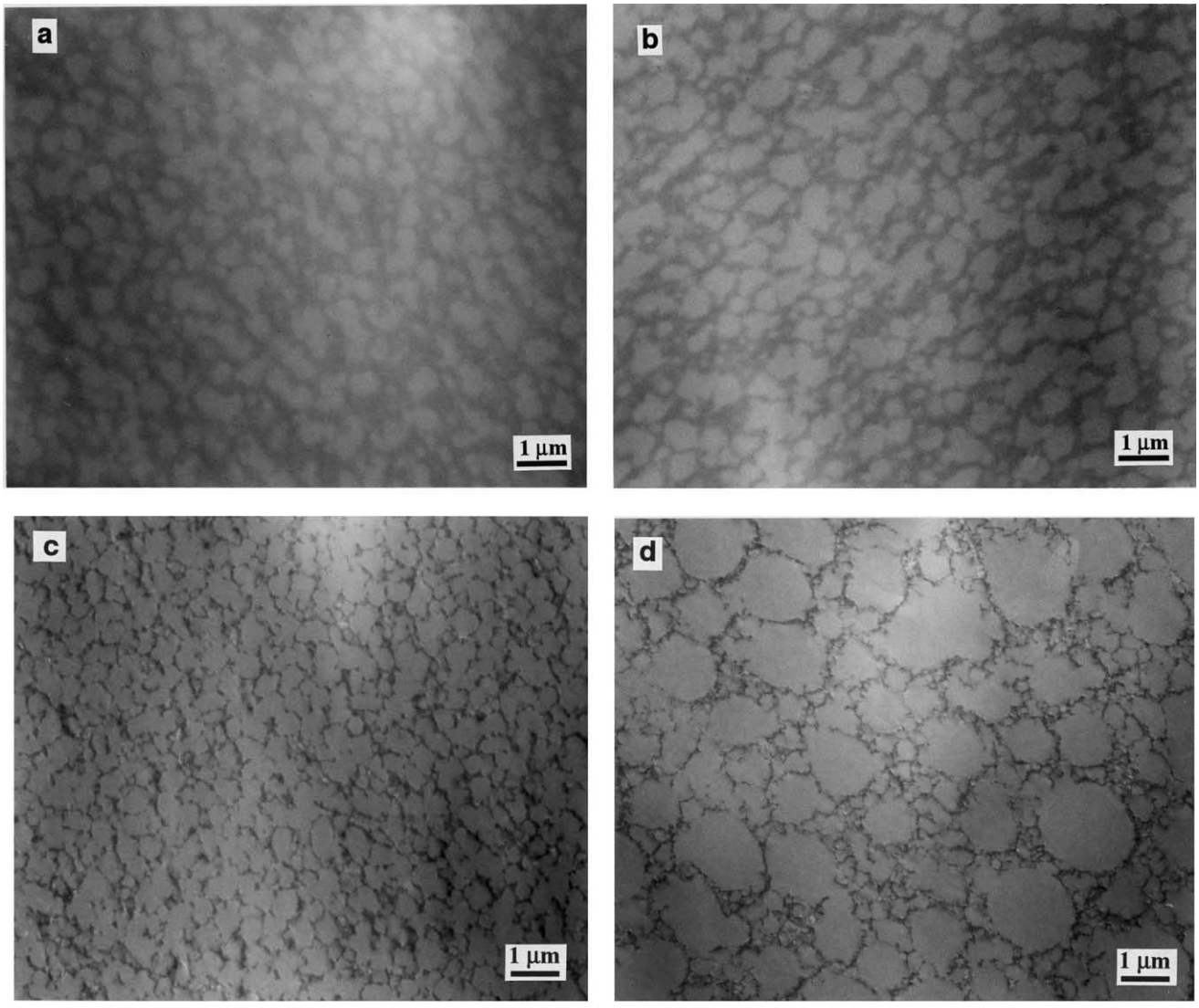

Fig. 17. Pattern evolution of phase separation during photopolymerization at 150 °C with a light intensity of 1 mW cm^{-2} for BPE4/PSU (9/1 w/w): (a) irradiation time = 37 s, (b) 45 s, (c) 60 s and (d) 180 s.

area in the blend at the early stage of phase decomposition, and the matrix area decreased with irradiation time. At the early stage of phase separation, the matrix phase should contain too many BPE4 molecules compared with PSU molecules due to the extremely asymmetric composition of 10 wt% PSU. However, the PSU composition in this matrix phase increases as the phase decomposition proceeds. Finally, this matrix phase literally develops into a PSU-rich phase. The network-like region of the PSU-rich phase became fairly thin in the blend after photoirradiation for 60 s compared with that of the blend at 45 s.

It is evident from Fig. 17 that the BPE4-rich domains were generated over various periods of time (t_{ir} = 30–90 s). The distribution curves of the normalized BPE4-rich domain in the TEM images are shown in Fig. 18. In the blend irradiated below 40 s, the domain sizes of the BPE4-rich phase gave mono-distribution curves with a main peak at around 0.5 μm, whereas the distribution curves were divided into two or three curves in the blend after irradiation for 45 s or more. The distribution curves at the low domain region give a peak at around 0.2 μm, which corresponds to the peaks of the small domains in the resulting phase structures (see Fig. 7). These domains were generated in the limited PSU-rich phase after 40 s, in the second step, when coatings were irradiated for longer periods. The domains in the distribution curves at the large domain region correspond to the saturated BPE4-rich domains formed at the beginning of phase decomposition. The maximums in these curves gradually shifted to the large domain region. In the TEM images, the PSU-rich network-like phase became thin as the BPE4-rich domains grew. The temporal change in q_m is shown in Fig. 19, where $q_m = R_m/2\pi$ was obtained from the peak of the distribution curve. BPE4-rich domains grow as $q_m \sim t^{-0.33}$ during phase separation from 37 to 90 s. The exponent factor (0.33) corresponds well to usual factor (1/6–1/3) predicted

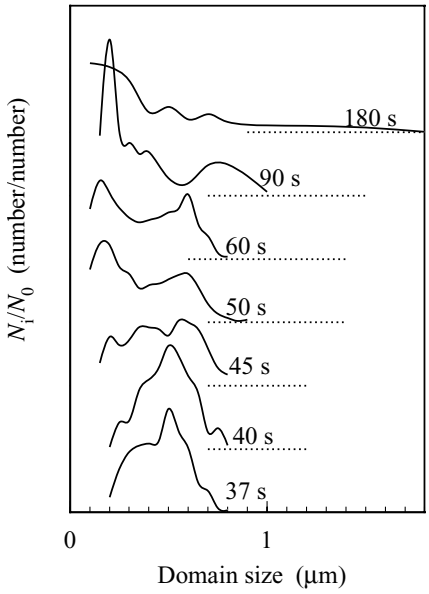

Fig. 18. Temporal changes in distribution curves of BPE4-rich domain size during photopolymerization for BPE4/PSU (9/1 w/w) cured at 150 °C with a light intensity of 1 mW cm^{-2}.

in the middle stage of phase decomposition in the spinodal mode. This exponent factor is higher than that of typical viscoelastic phase separation systems without chemical reaction [17]. However, large exponent values (0.5–1.1), which increase with curing temperature, are obtained in thermal polymerization-induced phase separation systems [9,10].

Fig. 20 shows a temporal change in the number density, which was obtained by the mean domain number in an area of 1 μm^2 in the TEM images. Most large domains, which occupied a major area in the blend, were formed within ca. 40 s of photoirradiation. The number density at 40 s of irradiation was ca. 3 (n μm^{-2}). The number density

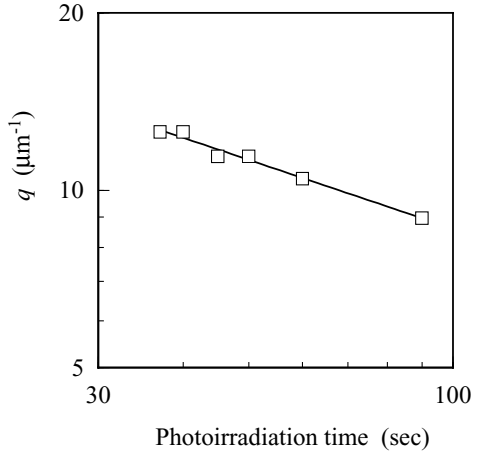

Fig. 19. Temporal change in q_m during phase decomposition from 37 to 90 s for BPE4/PSU (9/1 w/w) cured at 150 °C with a light intensity of 1 mW cm^{-2}; q_m ($= R_m/2\pi$) is the wave number of the BPE4-rich domain. R_m is the BPE4-rich domain size.

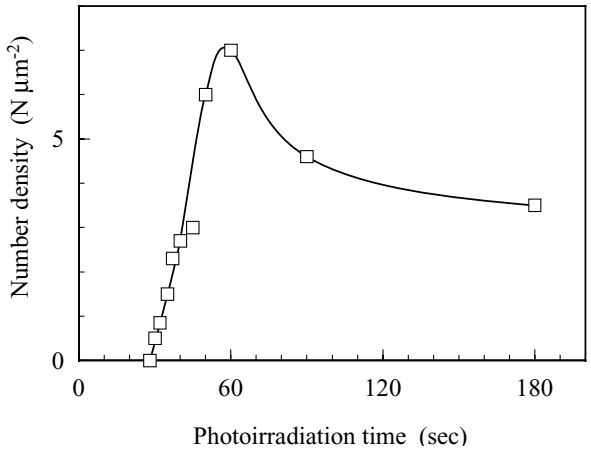

Fig. 20. Temporal change of number density in a blend of BPE4/PSU (9/1 w/w) during photopolymerization at 150 °C.

increased to 7 (n μm^{-2}) following photoirradiation for 40–60 s. The increase in the number density was mainly brought on by the small domains generated after ca. 40 s of irradiation or more. Incidentally, the number density for a close-packed structure with a diameter of 0.5 μm is ca. 4.6 (n μm^{-2}). This can be attributed to the polymerization-induced phase separation system, in which the polymerization (decreasing miscibility) and the phase separation proceed simultaneously.

The PSU-rich phase shrank and elongated with irradiation time (>90 s), and then the BPE4-rich domains coalesced at the same time that the PSU-rich phase partly broke down (see Fig. 17(d)). Eventually, a broken network-like structure appeared. Domain density decreased with the coalescence of a BPE4-rich domain. Similar phenomena have been reported in the polymer solution systems [15].

In the case of the standard light intensity of 10 mW cm^{-2},

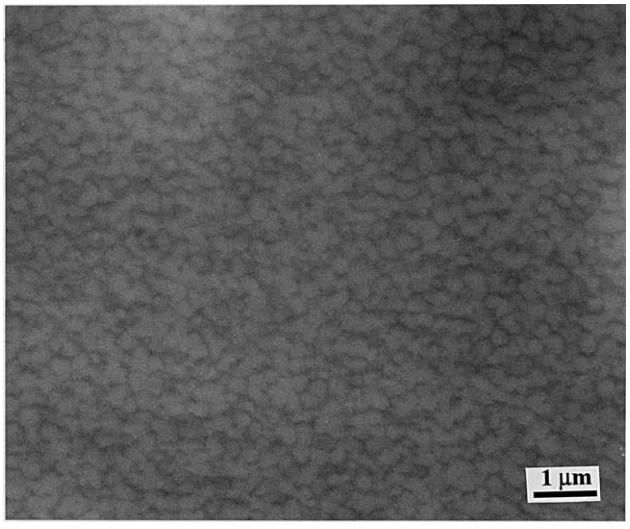

Fig. 21. Phase structure of BPE4/PSU (9/1 w/w) after photoirradiation at 120 °C for 3.2 s with a light intensity of 10 mW cm^{-2}.

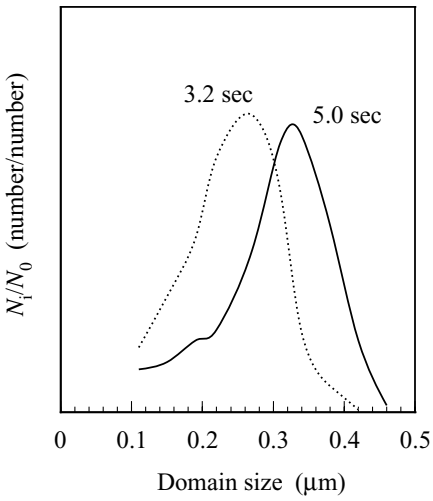

Fig. 22. Temporal change in distribution curves of BPE4-rich domain size during photopolymerization for BPE4/PSU (9/1 w/w) cured at 120 °C with a light intensity of 10 mW cm^{-2}.

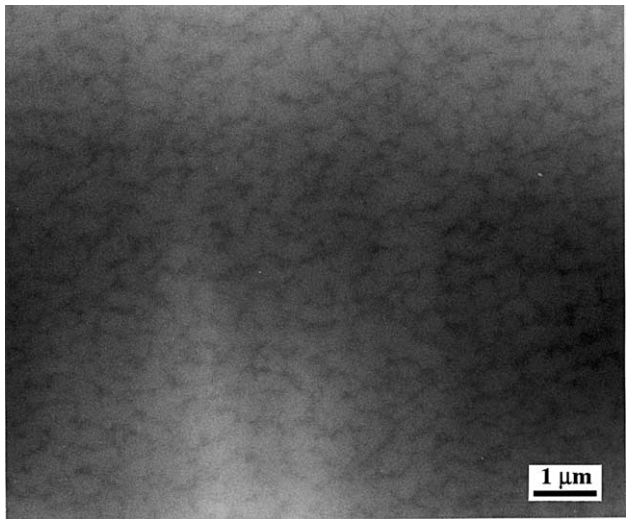

Fig. 23. Phase structure of BPE4/PSU (95/5 w/w) after photoirradiation at 80 °C for 25 s with a light intensity of 2 mW cm^{-2}. A clear network-like structure appeared.

phase decomposition proceeded very fast. The resultants are shown in Fig. 21 (TEM images) and Fig. 22 (distribution curves of BPE4-rich domain sizes). The blend with 10 wt% PSU content was photoirradiated at 120 °C. BPE4-rich domains with uniform size of 0.16 μm appeared in a PSU-rich matrix at the same time after a irradiation time of ca. 2.5 s. A network-like structure was gradually shaped with the growth of BPE4-rich domains. At 5 s of irradiation, the distribution curve corresponded well with that of the resulting structure in Fig. 7. A network-like phase separated structure was almost formed after only 5 s of photoirradiation at the standard light intensity.

A blend with 5 wt% PSU content, the resulting structure of which was the shred network-like structure, provided the network-like pattern at an early stage of phase decomposition. Fig. 23 shows a TEM image of the blend with 5 wt% PSU photoirradiated for 25 s. The sample was prepared at 80 °C with a light intensity of 2 mW cm^{-2}. The network-like structure appeared at the early stage of phase decomposition. The shred network-like bicontinuous structure was developed from the closed network-like structure by shrinking the network-like phase with further photoirradiating.

These unusual phase separation phenomena, in which droplet structures develop into bicontinuous network-like structures, have been reported as typical viscoelastic phase separation behavior [15–18,20]. Network-like structures appear as a long-lived transient gel due to viscoelastic effects in the polymeric phase. Glass transition behavior in the blends cured at different temperatures suggests that BPE4 droplets grow in a homogeneous mixture similar to what occurs in an unclear-growth phase separation mode.

3.4. Domain size in resulting network-like structures

BPE4-rich domains in the network-like structures develop via the following three steps, (1) generation and rapid growth in a polymeric-rich matrix, (2) slow growth and (3) coalescence. The effects of the second and third step growth decrease as light intensity increases. Based on the time-resolved observation, we consider that the domain sizes R_m in the resulting structures are roughly decided at the first step. The rapid growth of the domains should be slowed by entanglements of the polymeric phase, which in turn should be caused by the high concentration of the polymeric component bought on by the quick condensation. In high-temperature curing, a higher density of the entanglement points Z is needed for the entanglements, since the longest relaxation time τ_R becomes shorter. The density of the entanglement points Z is related to PSU concentration. It is assumed that all PSU molecules in domain concentrate at the surface of the spherical domain. When the BPE4-rich domain with a diameter $2r$ grows in the PSU matrix, the PSU concentration at the surface increases as $4\pi r^2\rho_0/((4/3)\pi r^2\rho_0) = 3r$, where ρ_0 is the PSU concentration in homogeneous mixture. The longest relaxation time τ_R is related as $\tau_R \sim Z^{-3}(\sim r^{-3})$ [28]. The temperature dependence of the longest relaxation time $\tau_R(T)$ can be given by $\tau_R(T) \sim \exp(\Delta E/kT)(\sim r^{-3})$ due to the high temperature region ($>T_{g0}$ + 80 °C), where ΔE is the activation energy and k is the Boltzmann's constant. The activation energy ΔE can be obtained from the relationship between the reciprocal absolute temperature T^{-1} and the logarithm of the horizontal shift factor (log a_T), where $a_T = \tau_R(T)/\tau_R(T_0)$ [29]. Fig. 24 shows the relationships between T^{-1} and log R_m and log $a_T^{-(1/3)}$, where R_m is the domain size of the BPE4-rich phase in Fig. 8. The shift factor a_T was obtained as the shifted frequency value along the frequency axis to get the master curve of the storage shear modulus $G'(\omega)$ for BPE4-monomer/PSU before photoirradiation according to the frequency–temperature superposition. Reference temperatures T_0 for the master curves were

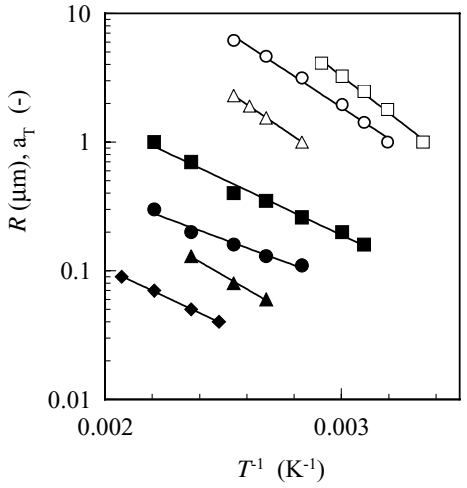

Fig. 24. Relationships between reciprocal absolute temperature (T^{-1}) and BPE4-rich domain sizes (R_m) (closed circle) and shift factor ($a_T^{-(1/3)}$) of $G'(\omega)$ (open circle) for BPE4/PSU: (□, ■) PSU = 10 wt%, (○, ●) PSU = 20 wt%, (△, ▲) PSU = 30 wt% and (◆) PSU = 50 wt%. Reference temperatures T_0 of a_T are 26 °C (10 wt% PSU), 40 °C (20 wt% PSU) and 80 °C (30 wt% PSU).

26 °C for 10 wt% PSU, 40 °C for 20 wt% PSU and 80 °C for 30 wt% PSU. Straight-line relationships are given. ΔEs obtained from the slopes in Fig. 24 are shown in Table 2. The activation energies ($\Delta E_a/3 = 2.5$–2.8) of the shift factors corresponds well to those ($\Delta E_d = 1.5$–2.0) of the domains.

On the other hand, at high light intensity, the phase separation rate becomes higher, which results in a longer τ_R (toward a lower Z), due to the high reaction rate. This is one of reasons that the domains decreased with light intensity. The relationship between reaction rate K and light intensity I is given by $K \sim I^{1/2}$ [26]. Phase separation rate V is assumed to be related to reaction rate K. Phase separation rate V corresponds to the longest relaxation time τ_R ($\sim r^{-3}$), and then the relation of $r(I) \sim r_0 I^{-(1/6)}$ can be obtained. The exponent factors in Fig. 11 are 0.34 at 120 °C and 0.42 at 150 °C. These experimental factors are higher than the calculated factor. This difference can be ascribed to the effect of the slow growth in the second step. The slow growth in the second step should further progress as the light intensity (reaction rate) decreases. The lower the light intensity, the larger the domains grow.

Table 2
Activation energies ΔE_d and ΔE_a obtained from domain size (R_m) in resulting structure and shift factor a_T of storage modulus G' of a homogeneous mixture, respectively

PSU (wt%)	ΔE_d from domain (kcal mol^{-1})	$\Delta E_a/3$ from a_T (kcal mol^{-1})
10	1.7	2.8
20	1.4	2.4
30	2.1	2.5
50	1.7	–

It has also been reported that domain size R_m is obtained as $R_m \sim K^{-(1/3)}$ in the blends associated with chemical reaction by the pinning effect [23,30].

4. Conclusions

The phase structure in a binary blend system of photocurable/linear polymers has been controlled by photopolymerization. Network-like bicontinuous phase separated patterns were formed by photopolymerization in a BPE4/PSU blend over a wide range of compositions of 5–70% by weight of PSU. In particular, the BPE4-rich domain size (characteristic length scale) in a network-like pattern varies from 0.03 to 1.0 μm under controlled processing conditions and blend composition, and transparent coatings were produced with domains below ca. 0.2 μm. The network-like morphologies developed with the increase and growth of BPE4-rich domains in a PSU-rich matrix via a viscoelastic phase separation mode. High performance or novel functional polymeric materials will be provided for photocurable polymer coatings by compounding the materials with a small amount of linear polymers, and small particles [15,31,32] and condensed molecules [15,31–33].

Acknowledgements

We would like to acknowledge the Analysis Center of Dainippon Ink and Chemicals (DIC), Inc., for their support of our experiments. We also wish to acknowledge helpful discussions and advice provided by Prof. T. Hideshima of Hokkaidou University. We wish to thank Dr S. Matsumoto, Dr N. Hayashi, Mrs K. Tanaka, and Mrs R. Kimura of the DIC, Inc., for discussions and advice on experimental measurements. We would like to thank Dr R-H. Jin and Dr A. Teramae of Kawamura Institute of Chemical Research for advice and comments.

References

[1] Inoue T. Prog Polym Sci 1995;20:119–53.
[2] Williams RJJ, Rozenberg BA, Pascault J-P. Adv Polym Sci 1997; 128:95–156.
[3] Venderbosch RW, Meijer HEH, Lemstra PJ. Polymer 1994;35(20): 4349–57.
[4] Jansen BJP, Meijer HEH, Lemstra PJ. Polymer 1999;40:2917–27.
[5] Chen J-L, Chang F-C. Macromolecules 1999;32(16):5348–56.
[6] Girard-Reydet E, Sautereau H, Pascault JP, Keates P, Navard P, Thollet G, Vigier G. Polymer 1999;39(11):2269–80.
[7] Oyanguren PA, Galante MJ, Andromague K, Frontini PM, Williams RJJ. Polymer 1999;40:5249–55.
[8] Su CC, Woo EM. Polymer 1995;36(15):2883–94.
[9] Chen W, Kobayashi S, Inoue T, Ohnaga T, Ougizawa T. Polymer 1994;35(18):4015–21.
[10] Chen W, Li X, Dong T, Jiang M. Macromol Chem Phys 1998; 199:327–33.

[11] Harismendy I, Del Rio M, Marieta C, Gavalda J, Mondragon I. J Appl Polym Sci 2001;80:2759.
[12] Girard-Reydet E, Vigier G, Pascault JP, Sautereau H. J Appl Polym Sci 1997;65:2433–45.
[13] Horiuchi S, Street AC, Ougizawa T, Kitano T. Polymer 1994; 35(24):5283–92.
[14] Pearson RA, Yee AF. Polymer 1993;34(17):3658–70.
[15] Tanaka H. J Phys Condens Matter 2000;12:R207–64.
[16] Tanaka H. Macromolecules 1992;25(23):6377–80.
[17] Tanaka H. Phys Rev Lett 1993;71(19):3158–61.
[18] Tanaka H. J Chem Phys 1994;100(4):5323–37.
[19] Fukahori Y, Mashita N, Wakana Y, Utsumomiya T. Polym Prepr Jpn 1998;47(11):2692–3.
[20] Tanaka H. Phys Rev Lett 1996;76(5):787–90.
[21] Okada M, Sakaguchi T. Macromolecules 1999;32(12):4154–6.
[22] Okada M, Fujimoto K, Nose T. Macromolecules 1995;28(6):1795–800.
[23] Tran-Cong Q. Structure and properties of multiphase polymeric materials. New York: Marcel Dekker, 1998. Chapter 6.
[24] Tran-Cong Q, Nagaki T, Nakagawa T, Yano O, Soen T. Macromolecules 1989;22(6):2720–3.
[25] Harada A, Tran-Cong Q. Macromolecules 1997;30(6):1643–950.
[26] Decker C. Prog Polym Sci 1996;21:593–650.
[27] Fox TG. Bull Am Phys Soc 1956;1:123.
[28] Doi M, Edwards SF. The theory of polymer dynamics. Oxford: Clarendon Press, 1986. Chapter 7.
[29] McCrum NG, Read BE, Williams ML. Anelastic and dielectric effects in polymeric solids. New York: Wiley, 1967.
[30] Glotzer SC, Stauffer D, Jan N. Phys Rev Lett 1994;72(26):4109–12.
[31] Tanaka H. Phys Rev E 1999;59(6):6842–52.
[32] Tanaka H, Araki T. Phys Rev Lett 2000;85(6):1338–41.
[33] Shinkai S, Murata K. J Mater Chem 1998;8(3):485–95.